

# Impact of Azimuthally Controlled Fluidic Chevrons on Jet Noise

Brenda S. Henderson<sup>1</sup> and Thomas D. Norum.<sup>2</sup>  
*NASA Langley Research Center, Hampton, VA, 23681*

**The impact of azimuthally controlled air injection on broadband shock noise and mixing noise for single and dual stream jets was investigated. The single stream experiments focused on noise reduction for low supersonic jet exhausts. Dual stream experiments included high subsonic core and fan conditions and supersonic fan conditions with transonic core conditions. For the dual stream experiments, air was injected into the core stream. Significant reductions in broadband shock noise were achieved in a single jet with an injection mass flow equal to 1.2% of the core mass flow. Injection near the pylon produced greater broadband shock noise reductions than injection at other locations around the nozzle periphery. Air injection into the core stream did not result in broadband shock noise reduction in dual stream jets. Fluidic injection resulted in some mixing noise reductions for both the single and dual stream jets. For subsonic fan and core conditions, the lowest noise levels were obtained when injecting on the side of the nozzle closest to the microphone axis.**

## I. Introduction

**F**LUIDIC chevrons use the injection of air, or some other fluid such as water, to reduce jet mixing noise and sometimes broadband shock noise. The impact of the injected flow on the jet plume appears to be very sensitive to injector configuration. Common configurations include slot injection where air at moderate pressure is injected through slots near the nozzle trailing edge and microjet injection where fluid is injected at high pressure through small tubes (with diameters often as small as 400 - 800 $\mu$ m) positioned slightly downstream of the nozzle trailing edge. The benefits of fluidic chevrons over passive devices such as mechanical chevrons (nozzles with trailing edge serrations that deflect into the flow) include deployment of the devices only during high noise operations and adjustment of the device operation to meet changing jet plume conditions throughout the flight envelope. Azimuthally controlled injection has the potential to reduce jet noise in installed configurations where flow asymmetries may significantly impact the resulting radiated noise and possibly reduce the amount of fluid needed for effective noise reduction. The current study investigates the impact of azimuthally-controlled fluidic chevrons on jet mixing noise and broadband shock noise produced by single and dual stream jets.

Noise sources within the jet plume include mixing noise for subsonic and supersonic exhausts as well as broadband shock noise and screech tones for supersonic exhausts. While mixing noise is present at all observation angles, it peaks in the downstream direction relative to the nozzle exit. Broadband shock noise resulting from interactions between stream disturbances and shock waves in the jet tends to dominate the acoustic spectra at upstream and broadside observation angles<sup>1,2,3</sup>. In dual stream jets, the production of broadband shock noise depends on the fan pressure relative to the core pressure due to the complicated shock cell structure in the flow<sup>4,5</sup>. Screech tones are commonly observed in acoustic spectra acquired at upstream and broadside observation angles of cold laboratory jets. Screech tones are part of a feedback loop where disturbances created at the nozzle lip interact with shocks in the jet shock-cell structure to produce sound (screech tones) which travels back to the nozzle lip to create further disturbances<sup>6</sup>.

The reduction of mixing noise using fluidic injection on subsonic jets has been shown previously for both single and dual stream configurations<sup>7,8,9</sup>. The impact of the injectors on the jet plume (and the noise sources within the jet) appears to depend on the injection configuration. Arakeri et al.<sup>10</sup> have shown microjet injection results in reduced turbulence intensities and an increased potential core length compared to the normal jet. Comparisons between flow fields produced by microjet injection and mechanical chevrons show significant differences in vortex development for the two noise reduction devices<sup>11</sup>. However, computational studies comparing slot injection and

---

<sup>1</sup> Senior Researcher, Aeroacoustics Branch, Mail Stop 166, AIAA Member.

<sup>2</sup> Senior Researcher, Aeroacoustics Branch, Mail Stop 166.

mechanical chevrons show significant reductions in potential core length over that of the normal jet for both devices<sup>12,13</sup>.

In supersonic jets, fluidic injection has been shown to reduce mixing noise and broadband shock noise. Reductions in both noise sources have been achieved for microjet and slot injection with single stream jets<sup>14,15,7</sup>. The reductions in broadband shock noise are presumably associated with modifications to the shock cell structure although there is little reported flow field data. The application of fluidic injection to dual stream (supersonic) jets is limited. The studies of Henderson and Norum<sup>14</sup> showed reductions in broadband shock noise and mixing noise for low supersonic conditions of the fan when injecting into the core stream. As the fan stream pressure increased, only mixing noise reduction was achieved. The studies did not include results for injection into the fan stream.

The experiments reported here investigate the impact of an azimuthally-controlled, core fluidic chevron on mixing noise and broadband shock noise for single and dual stream jets. Both subsonic and supersonic exhaust speeds are investigated.

## II. Experimental Approach

The experiments were conducted at NASA Langley Research Center in the Low Speed Aeroacoustics Wind Tunnel (LSAWT) shown in Fig. 1. The 56 inch x 56 inch square tunnel nozzle exhausts into a 34 ft long test cell with a 17 ft x 17 ft cross section, providing a simulated flight stream with a Mach number up to 0.32. The floor, ceiling, and walls of the test cell are covered with fiberglass wedges. The Jet Engine Simulator (JES), located in the center of the free jet, consists of co-annular streams used to simulate the exhaust of the fan and core streams of a turbo-fan engine. Each stream is equipped with an electric pre-heater and a propane-fired, sudden-expansion burner to achieve engine temperatures of commercial and military aircraft engines.

The acoustic results presented in this paper were obtained from the 28-element microphone sideline array located 12 ft from the centerline of the JES as shown in Fig. 1. Microphone calibrations including actuator and diffraction corrections have been made. In addition, the data have been corrected for shear layer effects using Amiet's<sup>16</sup> corrections and for absorption effects using the Shields and Bass<sup>17</sup> technique. The narrowband spectra have a bandwidth of 25.63 Hz and are presented for the FAA noise certification reference conditions (1 atm, 77°F, 70% relative humidity).

A representative 1/9<sup>th</sup> scale, bypass ratio (BPR) 5 nozzle system was used in the experiments. The baseline nozzles consisted of an externally plugged, 5.07 inch diameter core nozzle with an exit area of 10.98 in<sup>2</sup>, and a 9.45 inch diameter fan nozzle with an exit area of 29.14 in<sup>2</sup>. The baseline core nozzle had a uniform trailing edge thickness of 0.035". For the fluidic chevron investigations, this core nozzle was replaced with a fluidic chevron core nozzle. For the Generation II style fluidic chevron nozzle (Fig. 2), air was delivered to a common plenum in the core nozzle through an air delivery tube embedded in the pylon. Six contoured injection passages downstream of the plenum were used to deliver air to six slots cut on the core flow side of the nozzle near the nozzle trailing edge, creating a total of six fluidic chevrons. The Generation III fluidic chevron nozzle (Fig. 3) had four independently controlled air delivery tubes embedded in the pylon. Each of the four tubes delivered air to two contoured injection passages, one on each side of, and at equal distances from the pylon. The air was injected through a slot on the core flow side of the nozzle near the nozzle trailing edge. The injection angle of the Generation III nozzle was roughly 50° to the jet direction, slightly greater than that of the Generation II nozzle. The total slot injection area was the same for both nozzles. The

exteriors of the fluidic chevron nozzle were scalloped to increase the thickness of the nozzle in the regions of the injection passages. The pylon was at located at an angle of 122° to the microphone axis for all nozzle configurations tested.

The experimental operating conditions for the core and fan streams are shown in Table 1. The nozzle pressure ratio (NPR) is the ratio of the stream stagnation pressure to the pressure in the test cell, and the

**Table 1. Nominal Test Points for Single and Dual Stream Experiments**

NPR <sub>c</sub>	TTR <sub>c</sub>	NPR <sub>f</sub>	TTR <sub>f</sub>	Experiment
2.18	1.06	NA	NA	Single Low Supersonic Core Stream (M <sub>c</sub> = 1.12 - 1.16)
2.30	2.48	NA	NA	
1.56	2.66	1.75	1.16	Dual High Subsonic Streams (M <sub>c</sub> = 0.85, M <sub>f</sub> = 0.93)
1.61	2.13	2.24	1.05	Low Supersonic Fan Stream with Transonic Core Stream (M <sub>f</sub> = 1.14 - 1.18, M <sub>c</sub> = 0.85 - 1.11)
1.61	2.24	2.36	1.16	
1.82	2.13	2.24	1.05	
1.82	2.24	2.36	1.16	
2.04	2.36	2.24	1.05	
2.04	2.36	2.36	1.16	
2.17	2.44	2.36	1.16	

total temperature ratio (TTR) is the ratio of the stream total temperature to the test cell temperature. The subscripts c and f indicate core and fan stream quantities, respectively, and M is their jet Mach number. For the single stream conditions, the core nozzle was operated at supersonic speeds and the fan nozzle was operated at the temperature and pressure of the free jet. The dual stream experiments consisted of one representative aircraft takeoff condition, with subsonic exhaust speeds for both the core and fan streams, and a series of conditions consisting of supersonic fan exhaust speeds and a combination of subsonic and supersonic core speeds. All data presented in this paper were obtained at a simulated flight Mach number of 0.1.

Air injection properties were estimated using pressure, temperature, and mass flow measurements in the injection lines, along with some post test calibration measurements at the injection slots as shown in Fig. 4. These measurements allow for comparisons of acoustic changes with variations in air injection pressure ratio, total injected air mass flow, and total injected air momentum. Most of the comparisons in this paper are given in terms of the air injection line injection pressure ratio (LIPR), defined as the ratio of the pressure in the air supply line divided by the test cell ambient pressure. (The actual air injection pressure at the exit of the injection slots was determined to be slightly different for each of the 6 slots of the Generation II nozzle and for each of the 8 slots of the Generation III nozzle, but all were determined to be 90% +/- 5% of the air line injection pressure.) The Generation III nozzle allowed for measurements with azimuthal variations of injection, due to independent control of the four injection air lines of that nozzle. Hence four LIPR's are listed for the Generation III nozzle data, with the first LIPR being for the two chevrons closest to the pylon (see Fig. 3), and the last LIPR being for the two chevrons furthest from the pylon. Specification of a single LIPR indicates that all chevrons have the same injection pressure, whereas a missing LIPR or a LIPR = 1 indicates that there is no air injection.

### III. Results

Acoustic results are presented that show the influence of air injection into a single stream jet and into the core stream of dual stream jets. Presented first are the noise reductions due to air injection of both broadband shock noise and mixing noise for single supersonic jet exhausts. This is followed by the impact of fluidic chevrons on the mixing noise of dual stream subsonic jets. Finally, the inability of core stream injection with the Generation III nozzle to significantly influence the shock noise from dual streams consisting of a low supersonic fan stream surrounding either a subsonic or a supersonic core stream is demonstrated.

#### A. Single Low Supersonic Core Stream Results

The power spectra for the Generation III nozzle operated at  $NPR_c = 2.18$  with line injection pressure ratios up to 4.0 are shown in Fig. 5 for observation angles of  $61^\circ$  and  $147^\circ$ . Observation angles less than  $90^\circ$  are in the upstream direction. The upstream spectrum at LIPR = 1.0 exhibits a screech tone at about 2900 Hz that disappears with air injection, likely due to an interruption of the feedback loop at the nozzle exit. The broad peak in the spectrum at roughly 5500 Hz in Fig. 5(a) is caused by broadband shock noise, which is seen to decrease with increasing LIPR. However, the sound pressure levels at frequencies above 40,000 Hz increase slightly with increasing LIPR. In the downstream direction [Fig. 5(b)] where jet mixing noise is dominant, the peak mixing noise occurring at low frequencies is decreased only at the higher LIPR.

A comparison of the power spectra for the Generation II and III Air Injection nozzles operating at the same conditions used in Fig. 5 is shown in Fig. 6. The sound pressure levels of the broadband shock noise are the same for both nozzles despite the fact that the total injection mass flow rate of the Generation II nozzle is more than double that of the Generation III nozzle. This implies that increasing the injection mass flow rate at a given injection pressure has little effect on the broadband shock noise. Fig. 6(b) shows that in the downstream direction neither air injection nozzle operating at LIPR = 2.0 changes the mixing noise characteristics from the no injection case.

The impact of azimuthal variation in air injection on shock noise and mixing noise for the same jet conditions used in Figs. 5 and 6 is shown in Figs. 7 and 8. Figure 7 shows that the broadband shock noise peak decreases with an increase in the number of injection lines in operation at LIPR = 2.0. Figure 8 shows similar but not quite the same changes when the injection lines are activated in an order opposite to that shown in Fig. 7. The comparison between Figures 7 and 8 indicates that a single pair of injectors either close to or furthest from the pylon gives about the same reduction in the broadband shock noise, while the operation of four injectors closest to the pylon (injection lines 1 and 2) is more effective than operation of the four furthest from the pylon (injection lines 3 and 4).

The comparisons shown in Figs. 7 and 8 are repeated in Figs. 9 and 10, except that the LIPR has been increased from 2 to 4. In addition to the fact that the broadband noise levels are reduced by a larger amount at the higher LIPR, the noise reduction is much better with injection from the two lines closest to the pylon than with injection

from the two lines furthest from the pylon. A clear demonstration of this conclusion is seen in Fig. 11, which directly compares the noise reduction of injection from the upper two lines with that of the lower two lines.

A comparison of the downstream spectra in Figs. 7 to 11 show that air injection results in small decreases in the mixing noise, with this decrease becoming more visible as both the injection pressure and the number of active injector lines increase.

The power spectra for the Generation II and III nozzles at equal operating conditions and LIPR are shown in Fig. 12. The noise characteristics at both observation angles for the two nozzles are quite similar although the Generation II nozzle at LIPR = 4.0 has better high frequency noise characteristics in the peak jet noise direction than the Generation III nozzle at the same condition.

Figures 13 and 14 show the influences of injection mass and momentum on the upstream broadband shock noise and the downstream jet mixing noise, respectively. The injection conditions were chosen so that both the total mass and momentum of the injected air were kept constant, which was accomplished by increasing the pressure of the active injectors as the number of active injectors decreased. The constant mass and momentum of the three air injection cases in Figs. 13(a) and 14(a) are lower than those of Figs. 13 (b) and 14 (b). Figure 13 shows that, for both levels of constant mass and momentum, the reduction in the broadband shock noise peak is about the same, independent of the number of injection lines activated, but that this reduction is larger for the higher of the two mass flows. As shown in Fig. 13(b), a reduction of about 8 dB in the peak of the broadband shock noise occurs at a injection mass of 1.2% of the core mass flow. Figure 14 shows that for either mass flow air injection yields only minimal mixing noise reduction.

The second single jet condition tested was at a somewhat higher pressure (NPR = 2.30 vs 2.18) and a much higher temperature (TTR = 2.48 vs 1.06) than the first condition. Figure 15 shows the effects of air injection at this second condition at the same LIPR as was presented in Fig. 5 for the first condition. Because of the much higher jet temperature, the broadband shock noise peak is much less pronounced than in Fig. 5, and hence the shock noise is less affected by air injection. However, as in Fig. 5(a), the noise does decrease as the LIPR increases. Figure 15(b) shows the mixing noise decreasing with increasing LIPR by about the same amount as in Fig 5(b).

## B. Dual High Subsonic Streams Results

Impact of air injection on mixing noise produced by the Generation III nozzle at  $NPR_c = 1.56$  and  $NPR_f = 1.75$  is shown in Fig. 16. Because trailing edge noise can occur when the Generation III nozzle is operated with dual subsonic streams and no injection, the baseline nozzle data is used here for the no injector case. The first injection case shown in the figure consists of all injectors operating at an LIPR = 2.5, and the other case consists of three lines operating at LIPR = 1.5 and the line furthest from the pylon (and closest to the microphone array) at 2.5. The spectra in Fig. 16 (a) show that at an observation angle of  $90^\circ$  the high frequency noise is increased due to air injection. However, in the downstream peak noise direction shown in Fig 16(b), air injection noise reduction is attained over a wide frequency range.

One-third octave band spectra obtained from the data of Fig. 16 and scaled by a factor of 9 are shown in Fig. 17. The air injection results in third octave sound pressure level increases of up to 3 dB at high frequencies (above 4000 Hz) for observation angles near  $90^\circ$ , and decreases of up to 3 dB at low frequencies (below roughly 1000 Hz) in the peak jet noise direction. Estimated effective perceived noise level (EPNL) calculations were made for the three conditions of Fig. 17 (using an assumed flight Mach number of 0.28). The EPNL reductions from the baseline

**Table 2. Injection Rates and  $\Delta$ EPNL**

Injection Line				$\square$ EPNL (EPNdB)	Mass <sub>inject</sub> (% Core)
1	2	3	4		
Baseline				0	
2.5	2.5	2.5	2.5	-0.8	2.9
1.5	1.5	1.5	2.5	-1.0	1.6

for the two injection configurations are shown in Table 2 along with the air injection mass flow as a percent of the core mass flow. An EPNL reduction of about 1 EPNdB is obtained. Note that this reduction is not compromised when three of the four injector lines operate at a lower injection pressure, indicating that a savings of injected mass can occur with selected azimuthal variation in injection rates. The two injection configurations discussed here gave the lowest estimated EPNL of all configurations tested.

## C. Low Supersonic Fan Stream with Transonic Core Steam

Narrowband spectra with and without air injection for the Generation III nozzle are shown in Figs. 18 and 19 for  $NPR_f = 2.35$  and  $NPR_c = 1.61$  and 1.82, respectively. Other than for an increase in the broadband shock noise seen in Fig. 18, air injection had no significant effect on the spectra in either the upstream or downstream direction. Spectra for the lower fan pressure ( $NPR_f = 2.24$ ) with a barely supersonic core ( $NPR_c = 2.04$ ) are given in Fig. 20. The broadband shock noise peak no longer exists in the upstream direction for the baseline configuration, indicating

an interruption of the typical shock cell structure in the flow. The only effect of air injection on these spectra appears to be a slight decrease in the mixing noise in the downstream direction. In fact, no significant decrease in noise could be found with air injection for any of the seven conditions tested with a supersonic fan stream. Hence air injection into the core stream of a dual stream jet appears to be ineffective in reducing noise when the noise sources are dominated by a supersonic fan stream.

#### IV. Conclusions

Broadband shock noise reductions of up to 8 dB are achieved in a single stream jet with injection mass flow rates of 1.2% of the core mass flow. Injecting near the pylon produces lower broadband shock noise levels than injecting at other locations around the nozzle periphery. Equivalent shock noise reductions are achieved with the Generation II and III nozzles operating at the same injection pressure ratio despite the significantly different injection mass flow rates of the two nozzles. In contrast, fluidic injection with the Generation III nozzle in a dual stream configuration having a supersonic fan stream does not reduce broadband shock noise for any of the operating conditions tested. Evidently, injecting into the core stream has little impact on the shock cell structure when the fan stream is at a much higher pressure than the core.

At least slight reductions in jet mixing noise can be achieved with the Generation III nozzle for all three types of core/fan conditions tested. For the dual subsonic stream jets, the lowest effective perceived noise level is achieved for an injection configuration with a higher injection pressure on the side of the nozzle closest to the microphones.

#### References

- <sup>1</sup>Harper-Bourne, M. and Fisher, M., "The noise from shock waves in supersonic jets," *Proceedings of AGARD Conference on Noise Mechanisms*, AGARD, 1973.
- <sup>2</sup>Tam, C., "Stochastic model theory of broadband shock associated noise from supersonic jets," *J.Sound and Vib.*, Vol. 116, Pt. 2, 1987, pp. 265 - 302.
- <sup>3</sup>Tam, C., "Stochastic model theory of broadband shock associated noise from supersonic jets in flight," *J.Sound and Vib.*, Vol. 151, Pt. 1, 1991, pp. 131-147.
- <sup>4</sup>Bhat, T., Ganz, U., and Guthrie, A., "Acoustic & flow-field characteristics of shock-cell noise from dual flow nozzles," AIAA-2005-2929.
- <sup>5</sup>Tam, C., Pastouchenko, N., and Viswanathan, K., "Computation of shock cell structure of dual stream jets for noise prediction," AIAA-2008-27, 2008.
- <sup>6</sup>Powell, A., "On the mechanism of choked jet noise," *Proc. Royal Soc.*, B 66, 1953, pp. 1039 - 1056.
- <sup>7</sup>Greska, B., Krothapalli, A., Burnside, N., and Horne, W. "High-speed noise reduction using microjets on a jet engine," AIAA-2004-2969, 2004.
- <sup>8</sup>Henderson, B., Kinzie, K., Whitmire, J., and Abeysinghe, A., "Aeroacoustic improvements to fluidic chevron nozzles," AIAA-2006-2706, 2006.
- <sup>9</sup>Callender, B., Gutmark, E., and Martens, S., "A comprehensive study of fluidic injection technology for jet noise reduction," AIAA-2007-3608, 2007.
- <sup>10</sup>Arakeri, A., Krothapalli, A., Siddavaram, V., Alkisar, M., and Lourenco, L., "On the use of microjets to suppress turbulence in a Mach 0.9 axisymmetric jet," *J.Fluid Mech.*, Vol. 490, 2003, pp. 75 - 98.
- <sup>11</sup>Alkisar, M., Krothapalli, A., and Butler, G., "The effect of streamwise vortices on the aeroacoustics of a Mach 0.9 jet," *J.Fluid Mech.*, Vol. 578, 2007, pp. 139 - 169.
- <sup>12</sup>Kinzie, K., Henderson, B., Whitmire, J., and Abeysinghe, A., "Fluidic chevrons for jet noise reduction," *Proceedings of the 2004 International Symposium on Active Control of Sound and Vibration (ACTIVE 04)*, INCE/USA, Williamsburg, VA, 2004.
- <sup>13</sup>Henderson, B., Kinzie, K., Whitmire, J., and Abeysinghe, A., "Impact of fluidic chevrons on jet noise," AIAA-2005-2888, 2005.
- <sup>14</sup>Henderson, B., Norum T., "Impact of fluidic chevrons on supersonic jet noise," AIAA-2007-3595, 2007.
- <sup>15</sup>Greska, B., and Krothapalli, A., "Jet noise reduction using aqueous microjet injection," AIAA-2004-2971, 2004.
- <sup>16</sup>Amiet, R., "Correction of open jet wind tunnel measurements for shear layer refraction," *AIAA 2<sup>nd</sup> Aero-Acoustics Conference*, Hampton, VA., AIAA-75-532, 1975.
- <sup>17</sup>Shields, F. and Bass, H., "Correction A study of atmospheric absorption of high frequency noise and application to fractional octave bands of noise," NASA Contractor Report 2760, 1976.

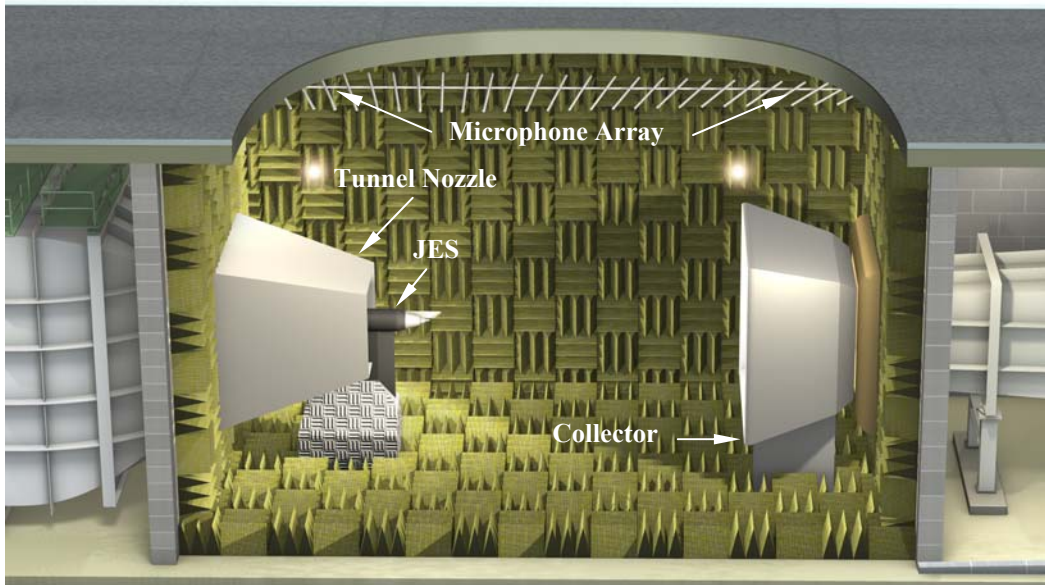


**Figure 1.** A schematic of the Low Speed Aeroacoustics Wind Tunnel (LSAWT) and the Jet Engine Simulator (JES).

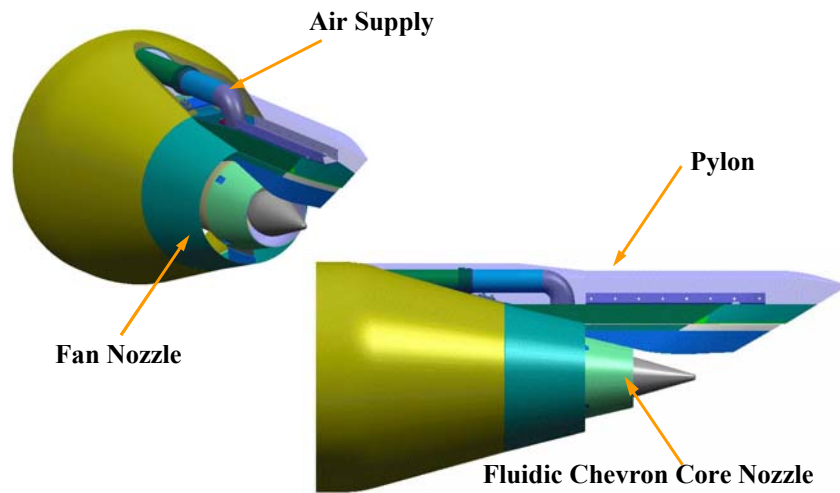


**Figure 2.** A schematic of the bypass ratio 5 nozzle system used in the experiments.

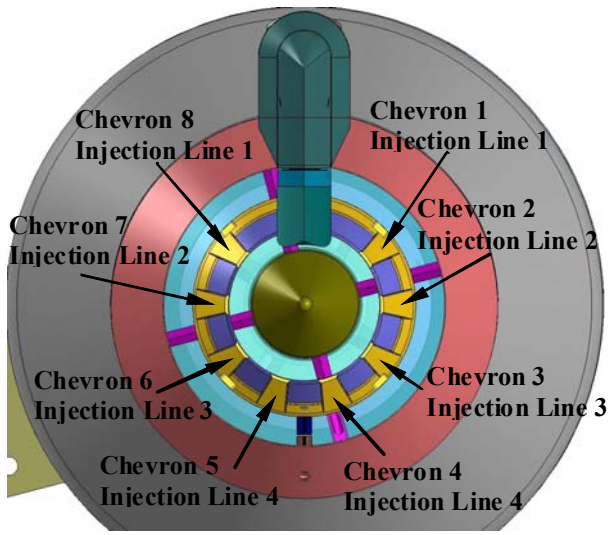


Figure 3. A solid model of the BPR 5 nozzle system with the Generation III (core) Air Injection nozzle.

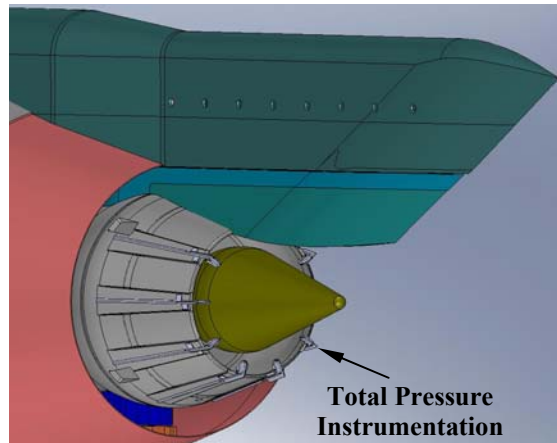


Figure 4. A solid model of the Generation III nozzle showing the calibration instrumentation for post-test pressure measurements.

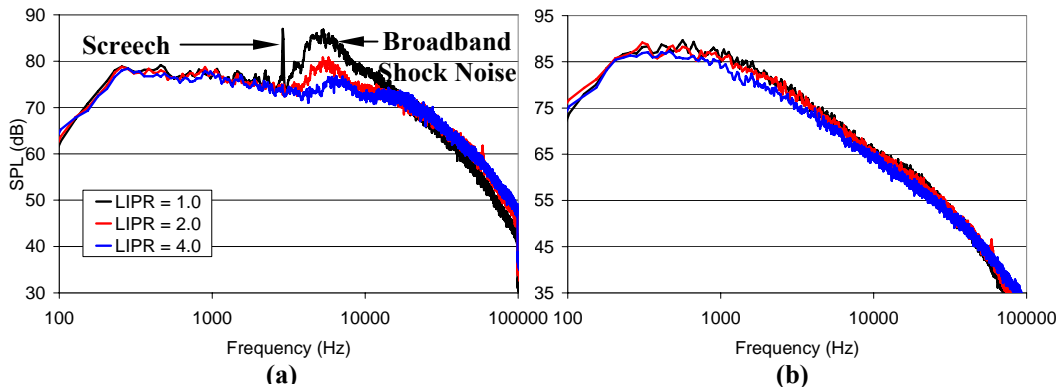


Figure 5. The narrowband power spectra for the single stream experiments using the Generation III nozzle at  $NPR_c = 2.18$ . For each dataset, all injectors were operated at the same LIPR. The observation angles are (a)  $61^\circ$  and (b)  $147^\circ$ .

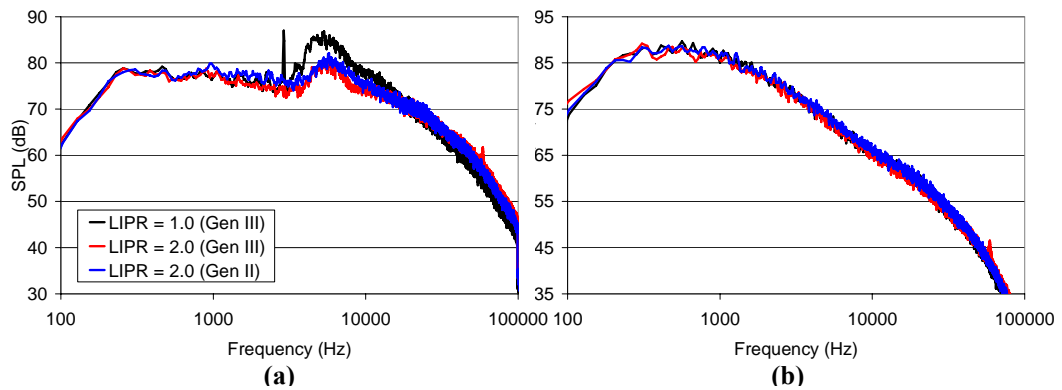
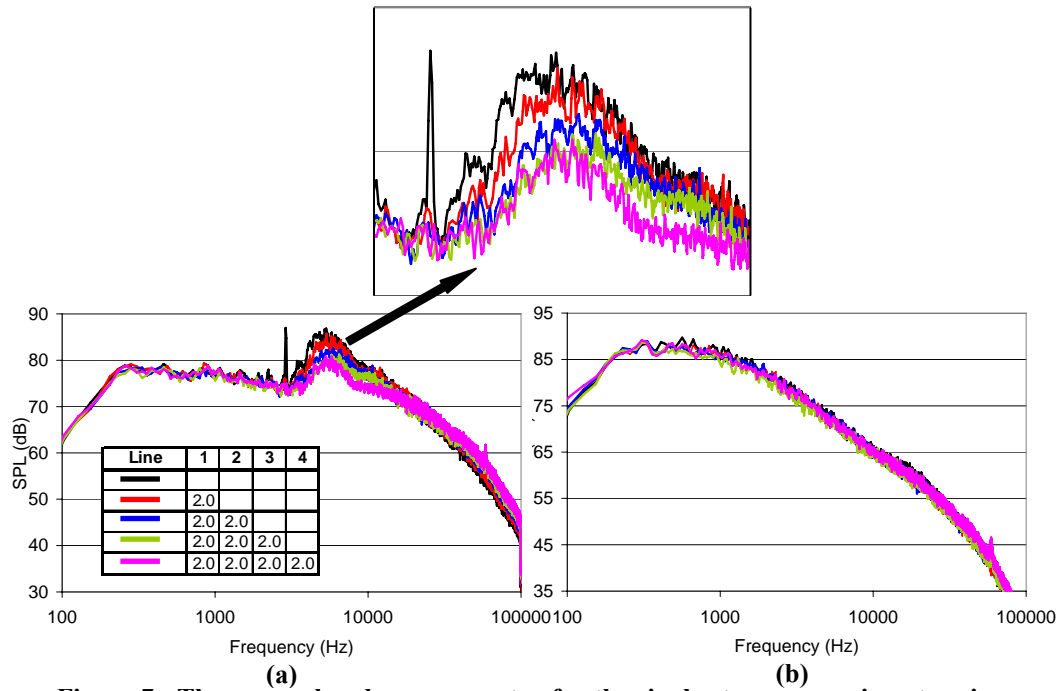
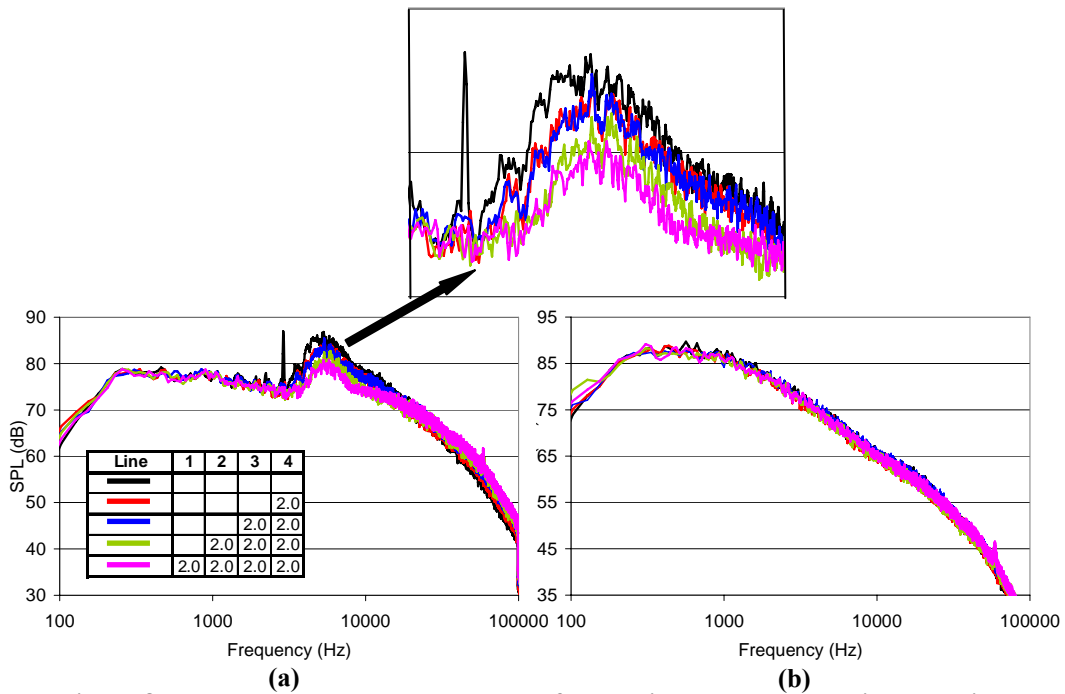


Figure 6. The narrowband power spectra for the single stream experiments and  $NPR_c = 2.18$ . For each dataset, all injectors were operated at the same LIPR. The observation angles are (a)  $61^\circ$  and (b)  $147^\circ$ .



**Figure 7. The narrowband power spectra for the single stream experiments using the Generation III nozzle at  $NPR_c = 2.18$ . The observation angles are (a)  $61^\circ$  and (b)  $147^\circ$ .**



**Figure 8. The narrowband power spectra for the single stream experiments using the Generation III nozzle at  $NPR_c = 2.18$ . The observation angles are (a)  $61^\circ$  and (b)  $147^\circ$ .**



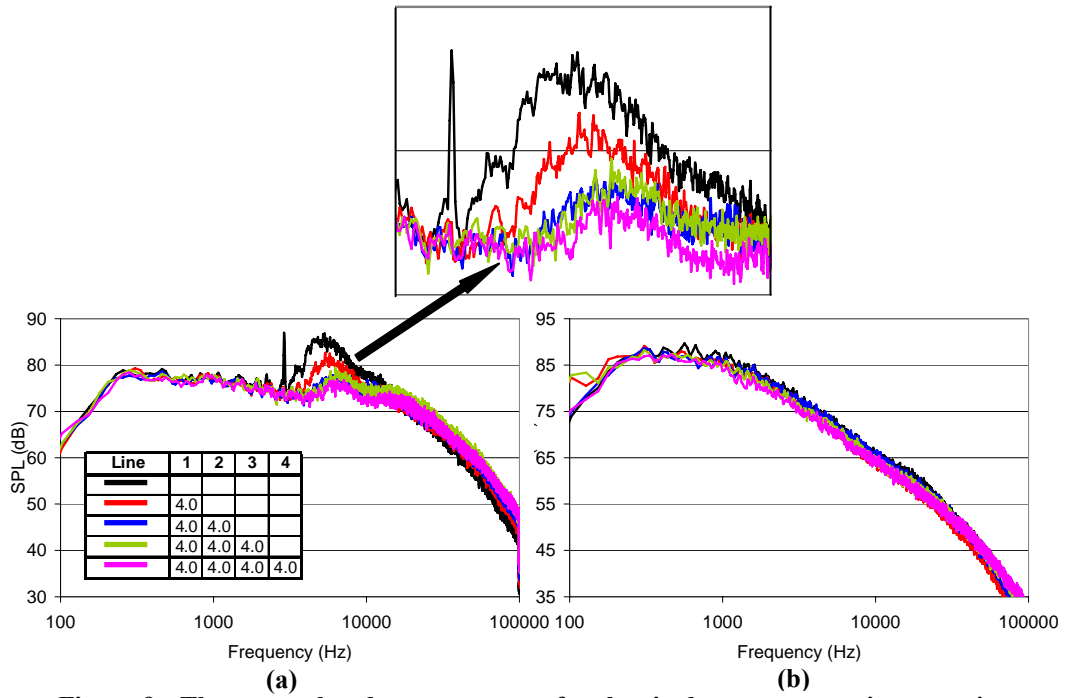


**Figure 9.** The narrowband power spectra for the single stream experiments using the Generation III nozzle at  $NPR_c = 2.18$ . The observation angles are (a)  $61^\circ$  and (b)  $147^\circ$ .

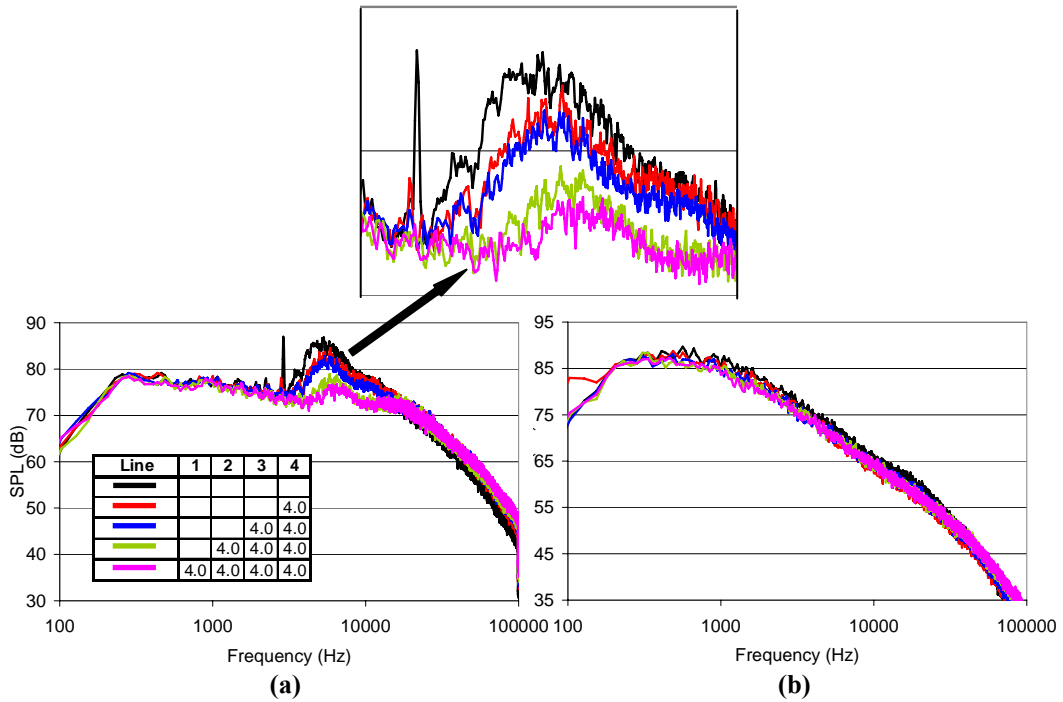


**Figure 10.** The narrowband power spectra for the single stream experiments using the Generation III nozzle at  $NPR_c = 2.18$ . The observation angles are (a)  $61^\circ$  and (b)  $147^\circ$ .

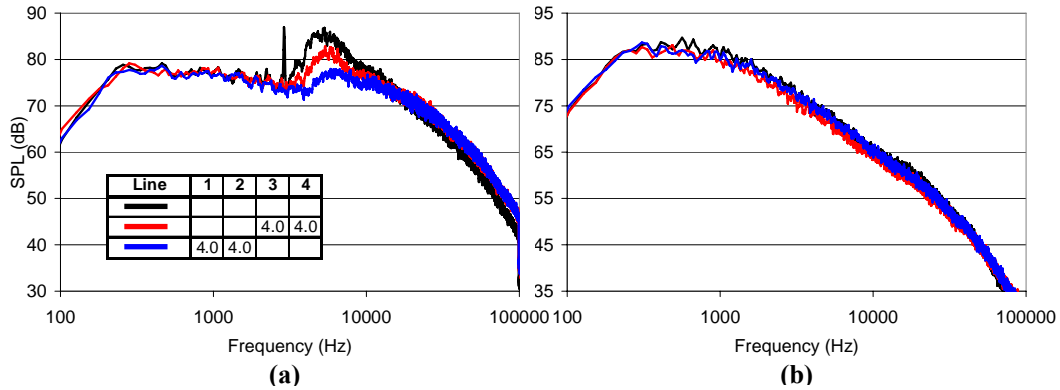


Figure 11. The narrowband power spectra for the single stream experiments using the Generation III nozzle at  $NPR_c = 2.18$ . The observation angles are (a)  $61^\circ$  and (b)  $147^\circ$ .

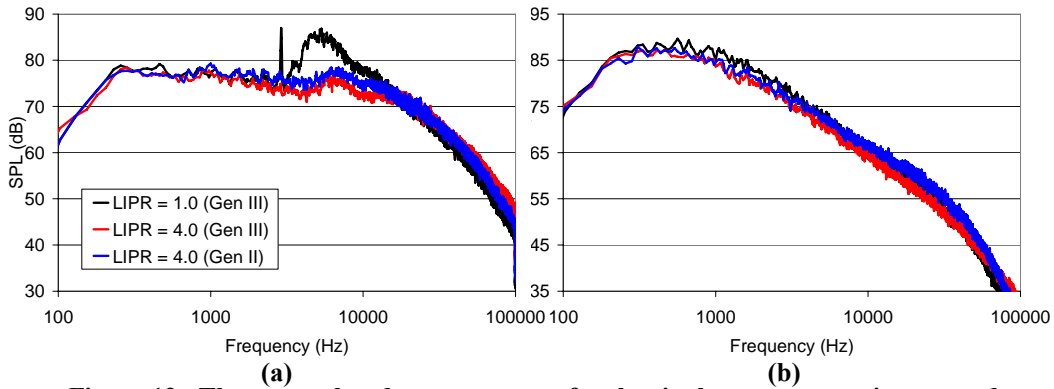


Figure 12. The narrowband power spectra for the single stream experiments and  $NPR_c = 2.18$ . For each dataset, all injectors were operated at the same LIPR. The observation angles are (a)  $61^\circ$  and (b)  $147^\circ$ .

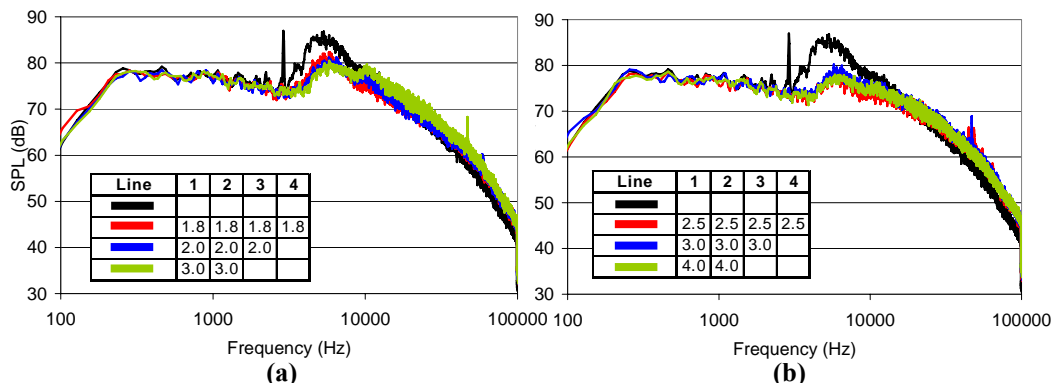
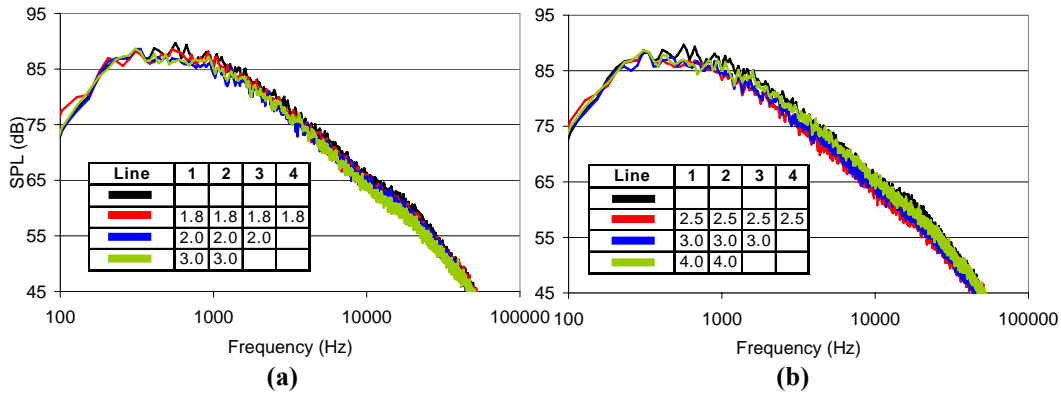
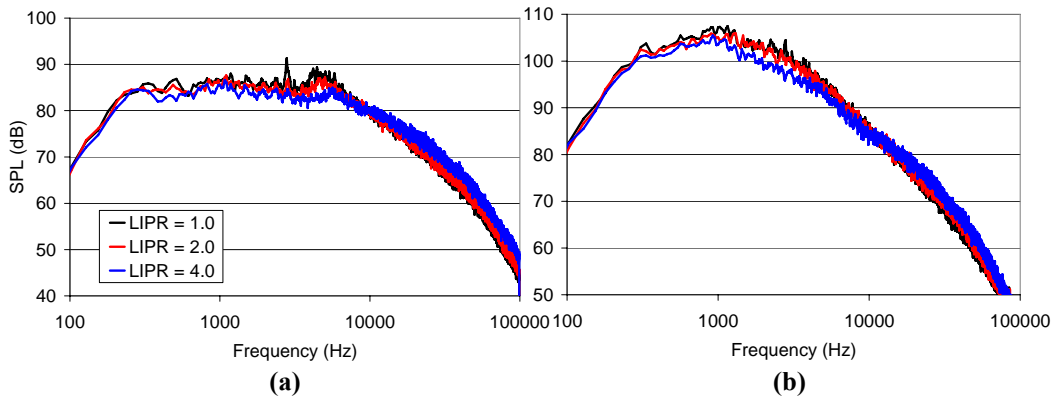


Figure 13. The narrowband power spectra for the single stream experiments at  $NPR_c = 2.18$  and an observation angle of  $61^\circ$ . In each plot, the datasets (except the baseline data) have an equal injection mass flow rate and an equal momentum flux. The injection mass flow rate in (a) is 0.7% and (b) 1.2% of the core flow rate.



**Figure 14.** The narrowband power spectra for an observation angle of  $147^\circ$  and the same operating conditions as those in Fig. 13. In each plot, the datasets (except the baseline data) have an equal injection mass flow rate and an equal momentum flux. The injection mass flow rate in (a) is 0.7% and in (b) is 1.2% of the core flow rate.



**Figure 15.** The narrowband power spectra for the single stream experiments using the Generation III nozzle at  $NPR_c = 2.30$ . For each dataset, all injectors were operated at the same LIPR. The observation angles are (a)  $61^\circ$  and (b)  $147^\circ$ .

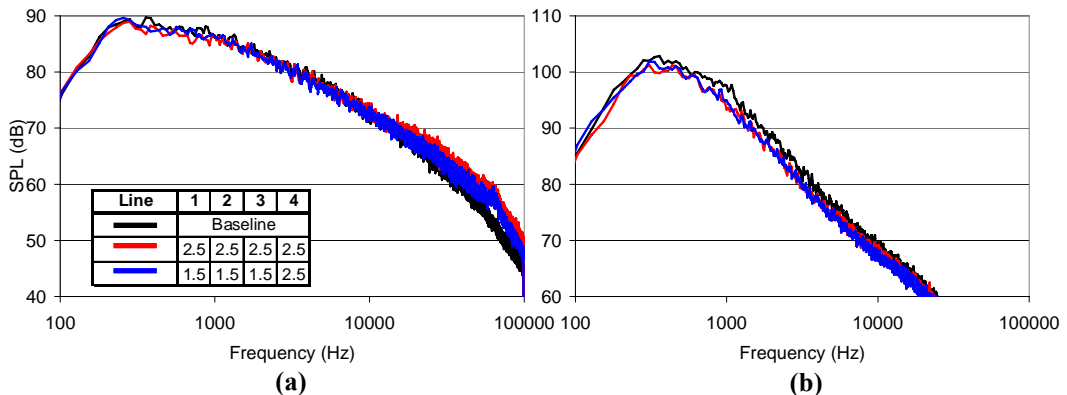


**Figure 16.** The narrowband power spectra for the dual high subsonic stream experiments ( $NPR_f = 1.75$  and  $NPR_c = 1.56$ ) using the Generation III Air Injection. The observation angles are (a)  $90^\circ$  and (b)  $147^\circ$ .

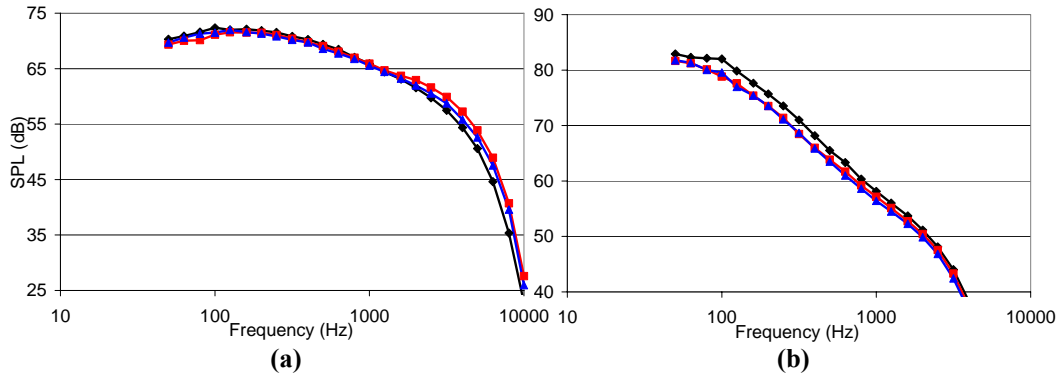


Figure 17. One-third octave band, scaled (using a scale factor of 9) data for the conditions in Fig. 16. The observation angles are (a)  $90^\circ$  and (b)  $147^\circ$ .

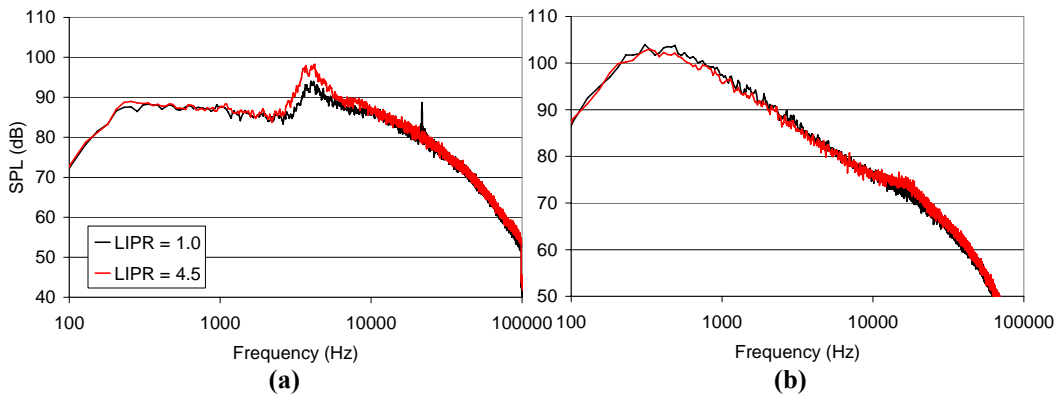


Figure 18. The narrowband power spectra for the dual stream experiments with supersonic fan conditions ( $NPR_f = 2.36$  and  $NPR_c = 1.61$ ) using the Generation III Air Injection nozzle. The observation angles are (a)  $61^\circ$  and (b)  $147^\circ$ .

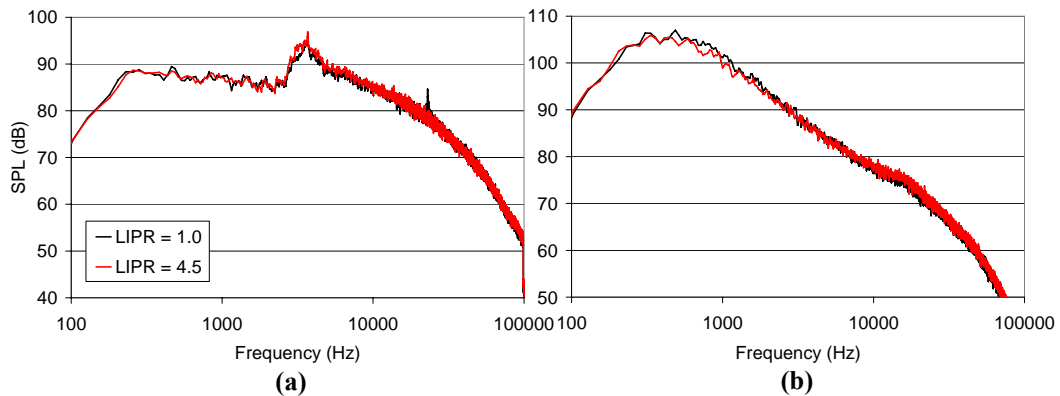
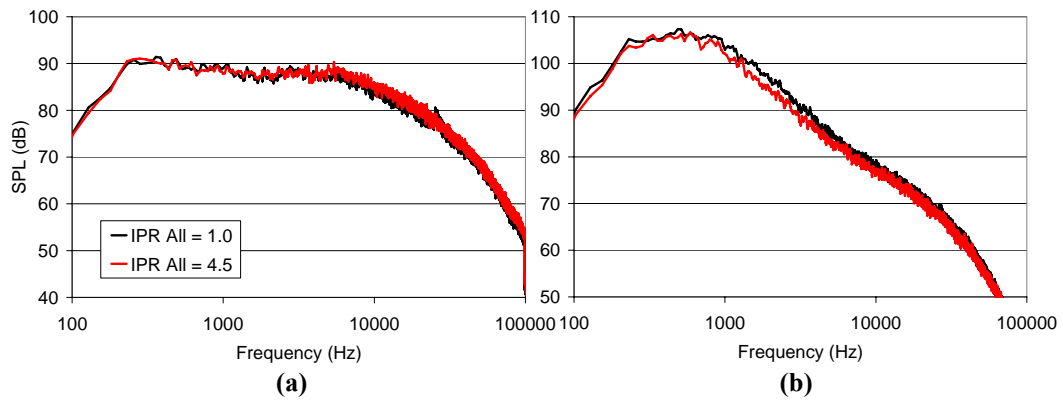


Figure 19. The narrowband power spectra for the dual stream experiments with supersonic fan conditions ( $NPR_f = 2.36$  and  $NPR_c = 1.82$ ) using the Generation III Air Injection nozzle. The observation angles are (a)  $61^\circ$  and (b)  $147^\circ$ .



**Figure 20. The narrowband power spectra for the dual stream experiments with supersonic fan conditions ( $NPR_f = 2.24$  and  $NPR_c = 2.04$ ) using the Generation III Air Injection nozzle. The observation angles are (a)  $61^\circ$  and (b)  $147^\circ$ .**